JOURNAL OF GEOPHYSICAL RESEARCH, VOL. 112, D10S08, doi:10.1029/2006JD007574, 2007

Ammonia sources, transport, transformation, and deposition in coastal New England during summer

Allen M. Smith,[1,2] William C. Keene,[1] John R. Maben,[1] Alexander A. P. Pszenny,[3,4] Emily Fischer,[4,5] and Andreas Stohl[6]

Received 29 May 2006; revised 22 November 2006; accepted 4 January 2007; published 11 May 2007.

[1] During summer 2004, NH_3, size-resolved particulate NH_4^+, and associated characteristics of surface air were measured continuously on Appledore Island, off the southern Maine coast as part of the International Consortium for Atmospheric Research on Transport and Transformation (ICARTT). NH_3 concentrations ranged from <0.6 to 123 nmol m^{-3} with maxima around local noon and minima near dawn. Particulate NH_4^+ ranged from 10.3 to 191 nmol m^{-3}. The transport of emissions from intensive agricultural activities in the eastern United States was an important source of total NH_3 ($NH_3 + NH_4^+$) over the Gulf of Maine during summer. Under cleaner northwest flow, total NH_3 concentrations were relatively low (median = 50.0 nmol m^{-3}) and partitioned roughly equally between phases; under the more polluted midwest flow, total NH_3 concentrations were substantially higher (median = 171 nmol m^{-3}) but dominated by particulate NH_4^+. Because particulate NH_4^+ was associated primarily with the highly acidic sub-μm size fractions with low deposition velocities (median flux = 1.5 μmol m^{-2} day^{-1}), dry-deposition fluxes were dominated by the gas phase (median = 6.2 μmol m^{-2} day^{-1}). Consequently, phase partitioning with pollutant-derived sulfur aerosol substantially increased both the atmospheric lifetime of total NH_3 against dry deposition and the relative importance of removal via wet- versus dry-deposition pathways. Total NH_3 accounted for 32% of the dry-deposition flux of inorganic N to the Gulf of Maine during summer. The combined dry deposition of total NH_3 and wet deposition of NH_4^+ via precipitation contributed 40% of the corresponding total atmospheric N flux.

Citation: Smith, A. M., W. C. Keene, J. R. Maben, A. A. P. Pszenny, E. Fischer, and A. Stohl (2007), Ammonia sources, transport, transformation, and deposition in coastal New England during summer, *J. Geophys. Res.*, *112*, D10S08, doi:10.1029/2006JD007574.

1. Introduction

[2] Globally, the anthropogenic production of reactive nitrogen (N) has increased by a factor of 10 over the last hundred years and is expected to increase by an additional factor of 2 over the next 50 years [*Galloway et al.*, 2004]. Increased emissions have resulted in a greater atmospheric burden of fixed nitrogen and associated increases in atmospheric deposition to the northeastern United States (US) [*Galloway et al.*, 1984]. Atmospheric deposition is one of the principal pathways by which nitrogen enters coastal waters along the eastern and southern US. *Castro et al.* [2001] estimate that wet deposition of inorganic nitrogen and the dry deposition of total NO_3 (gaseous HNO_3 + particulate NO_3^-) from the atmosphere contributes from 7% to 60%, or about 20% on average, to the total nitrogen loads to 42 coastal bays and estuaries along the Atlantic and Gulf coasts of the eastern U.S. Because this analysis does not account for the dry deposition of gaseous NH_3 and particulate NH_4^+, the estimated relative contributions of atmospheric inputs are considered lower limits. Surface waters in many coastal regions are nitrogen limited and, consequently, exogenous inputs of pollutant nitrogen can lead to excess phytoplankton production and associated degradation of ecosystems [*Nixon*, 1995; *Paerl*, 1985, 2002; *Larsen et al.*, 2001; *Paerl et al.*, 2002]. Deposition fluxes of atmospheric nitrogen are typically greatest during summer when surface coastal waters are often nitrogen limited and consequently sensitive to exogenous nitrogen inputs [*Scudlark and Church*, 1999; *Walker et al.*, 2004].

[3] Ammonia is emitted from numerous natural and anthropogenic sources (Table 1). Natural sources include volatilization from the plant-soil system, which varies as functions of soil type, pH, and temperature. Forests account for 20% to 40% of the NH_3 emissions in Maine and New Hampshire [*Langford et al.*, 1992]. Ammonia is also emitted from animal excreta, decomposing vegetation, wildfires,

[1]Department of Environmental Sciences, University of Virginia, Charlottesville, Virginia, USA.
[2]Now at Pollard Environmental, LLC, Richmond, Virginia, USA.
[3]Institute for the Study of Earth, Oceans, and Space, University of New Hampshire, Durham, New Hampshire, USA.
[4]Mount Washington Observatory, North Conway, New Hampshire, USA.
[5]Now at Department of Atmospheric Sciences, University of Washington, Seattle, Washington, USA.
[6]Norwegian Institute for Air Research, Kjeller, Norway.

0148-0227/07/2006JD007574$09.00

Table 1. Estimated Global Emissions of NH_3 in 1993 [Modified From *Galloway et al.*, 2004]

Source	Tg N yr^{-1}
Anthropogenic: Food	
Savannah burning	1.8
Agricultural waste burning	1.4
Deforestation burning	1.4
Fertilizers	9.7
Agricultural animal waste	22.9
Humans, pets and water waste	3.1
Agricultural crops	4.0
Subtotal	44.3
Anthropogenic: Energy	
Fossil fuel burning	0.1
Industrial processes	0.2
Biofuel consumption	2.6
Subtotal	2.9
Natural	
Soils and vegetation	4.6
Ocean	5.6
Subtotal	11.0
Total	58.2

and the surface ocean. Globally, natural sources of NH_3 are relatively less important than anthropogenic sources [*Galloway et al.*, 2004]. Biomass burning (both natural and anthropogenic) accounts for about 14% of the total global flux. The major anthropogenic sources of NH_3 in eastern North America are agriculture (animal waste [60%] and chemical fertilizers [16%]), human breath and perspiration (7%), domestic animals (7%), sewage treatment plants and septic systems (6%), industrial point sources (2%), and mobile sources (2%) [*Strader et al.*, 2004]. Since natural and anthropogenic sources of NH_3 vary spatially over eastern North America and the western North Atlantic Ocean, relative contributions from different sources and associated atmospheric concentrations in coastal New England vary as a function of transport region [*Parrish et al.*, 1993; *Driscoll et al.*, 2003].

[4] On the basis of its thermodynamic properties (Henry's law and dissociation constants), NH_3 partitions primarily with acidic sub-μm aerosol size fractions as a function of the pH and the volume of aerosol liquid water. Consequently, NH_3 phase partitioning in coastal New England is also influenced by the relative amounts of highly acidic sulphate aerosol (a reaction product of upwind pollutant SO_2 emissions) with which NH_3 chemically interacts. Phase partitioning has potentially important implications for the atmospheric lifetime of total NH_3; gaseous NH_3 has a typical atmospheric lifetime against dry deposition of less than a day whereas sub-μm aerosols, with which most particulate NH_4^+ is associated, have lifetimes on the order of many days [*Dentener and Crutzen*, 1994]. Ammonia may also react with gaseous H_2SO_4 and H_2O to form new particles [*Korhonen et al.*, 1999; *Kulmala et al.*, 2000].

[5] The sinks for total NH_3 in air are wet, cloud-water, and dry deposition to the surface. Wet-deposition fluxes have been reliably quantified by numerous programs [e.g., *Meyers et al.*, 2001]. In contrast, dry-deposition fluxes are associated with substantially greater uncertainties and relatively few estimates are available. Dry fluxes are typically modeled on the basis of measured concentrations of gaseous NH_3 and size-resolved particulate NH_4^+, the nature of the receiving surface (ocean, forest, grass, etc.), and associated meteorological conditions (wind velocity, relative humidity, and temperature) [e.g., *Hummelshøj et al.*, 1992; *Valigura*, 1995]. On average, the dry-deposition flux of atmospheric N to the mid-Atlantic coastal ocean during summer accounts for 43% of the total (wet + dry) deposition flux; NH_3 corresponds to 60% of the dry N flux [*Russell et al.*, 2003]. In contrast, *Jordan and Talbot* [2000] estimated that dry deposition to the coastal Gulf of Maine contributes only 10% to 20% of the total deposition flux of atmospheric N. However, their analysis did not consider the direct deposition of NH_3 vapor and, consequently, may have underestimated the relative contribution of dry deposition.

[6] During the summer of 2004, the chemical and physical evolution of polluted air along the New England coast was investigated from surface, aircraft, and ship platforms as part of the ICARTT campaign. On the basis of a subset of data generated under the auspices of Chemistry of Halogens at the Isles of Shoals (CHAiOS) ICARTT, this study evaluated the major processes that control the cycling of NH_3 and particulate NH_4^+ over coastal New England and the associated deposition fluxes to the Gulf of Maine.

2. Methods

2.1. Site Description

[7] Between 6 July and 12 August 2004, air was sampled on Appledore Island, Isles of Shoals, approximately 10 km off the coast of New Hampshire and Maine, USA (42.90°N,

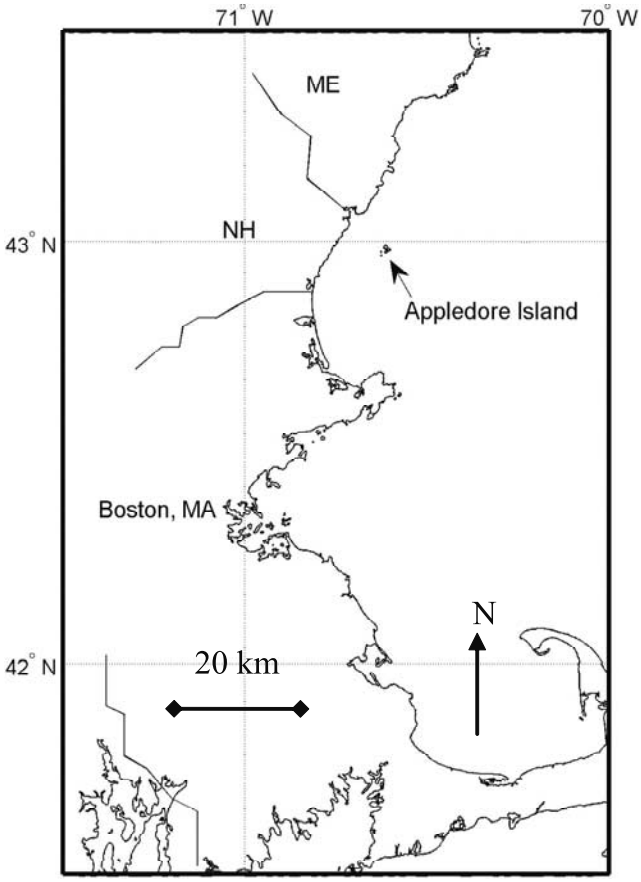

Figure 1. Location of sampling site.

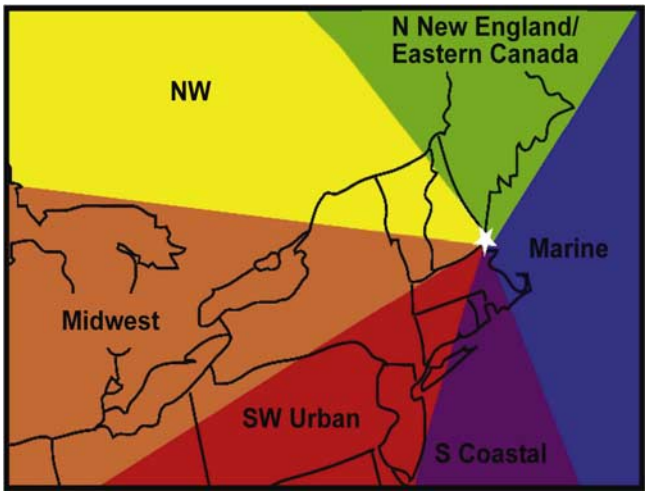

Figure 2. Major air mass source regions inferred from back trajectories and retroplumes.

70.62°W, Figure 1). Sampling equipment was installed on top of a World War II-era surveillance tower 43 m above the ocean surface. Samples were processed in a laboratory about 150 m from the tower.

2.2. Measurement Techniques

[8] Size-resolved aerosols were sampled over discrete daytime (~15 hours) and nighttime (~9 hours) periods using modified (with the addition of a top "0" stage) Graseby Anderson model 235 high-volume (about 1 m^3 min^{-1}) cascade impactors configured with Lexan (frosted polycarbonate) substrates and quartz back-up (Pallflex 2500 QAT_UP) filters. Bulk aerosol was sampled in parallel on a 20.3-by-25.4-cm quartz filter at an average flow rate of 1.2 m^3 min^{-1}. Average 50% aerodynamic cut diameters for the impaction stages were 18, 9.9, 3.9, 2.2, 1.1, and 0.56 μm, which yielded average geometric mean diameters (GMDs) for the size-resolved samples of 25, 13, 6.2, 2.9, 1.5, 0.77, and 0.39 μm. Immediately after recovery, substrates and filters were halved in a class-100 clean bench, transferred to clean polyethylene bags, sealed in glass Mason jars, and frozen. After the campaign, samples were transported frozen to Mount Washington Observatory, extracted in 18 Ω deionized water (DIW) and analyzed by ion chromatography (IC) for NH_4^+, NO_3^-, SO_4^{2-}, Cl^-, Na^+, and other major ionic constituents [*Pszenny et al.*, 2004; *Fischer et al.*, 2006]. Sea-salt (ss) and non-sea-salt (nss) constituents were differentiated using Na^+ as a sea-salt referencing species [*Keene et al.*, 1986].

[9] Gaseous NH_3, HNO_3, HCl, and other soluble reactive trace gases were sampled in parallel over two-hour intervals with tandem mist chambers containing DIW [e.g., *Keene et al.*, 2004]. Sample air was drawn through a size-fractioning inlet that inertially removed super-μm aerosols; sub-μm aerosols were removed downstream with an inline Teflon filter [*Keene et al.*, 1993]. Samples were analyzed by IC on site, usually within 12 hours of collection.

2.3. Meteorological Conditions and Surface Ocean Temperature

[10] Local air temperature and relative humidity (RH) were recorded at the Isles of Shoals, NH, meteorological station (IOSN3) operated by National Oceanic and Atmospheric Administration (NOAA). The station is located on White Island approximately 2.8 km S of the sampling site. Sea surface temperature was measured at two buoys (44013 and 44007) operated by NOAA's National Data Buoy Center that were moored 87 km S and 80 km NE, respectively, of the sampling site.

2.4. Regional Transport and Air Mass History

[11] Large-scale atmospheric transport was evaluated using both HYbrid Single-Particle Lagrangian Integrated Trajectory (HYSPLIT) back t rajectories [*Draxler and Rolph*, 2005] and Lagrangian particle dispersion (FLEXPART) retroplumes [*Stohl et al.*, 2005]. HYSPLIT trajectories were calculated every 6 hours (0, 6, 12, and 18 UTC) and archived by the Plymouth State Weather Center (http://pscwx.plymouth.edu/ICARTT/archive.html). FLEXPART was run in backward mode [*Stohl et al.*, 2003; *Seibert and Frank*, 2004]. Every 3 hours, 40,000 particles were released from the location of the measurement site and followed backward in time for 20 days to form so-called retroplumes. The retroplume model output consists of emission sensitivities, which were plotted both as atmospheric column-integrated values to visualize the overall transport, and as footprint values. The footprint is the emission sensitivity in the lowest model output layer (0–150 m above the surface) since most of the emissions occur near the ground. Therefore the footprint indicates the potential for emission uptake for the sampled air mass. Transport to Appledore over the course of the experiment was categorizing into six regional flow sectors based on visual inspection of the HYSPLIT trajectories and the FLEXPART column-integrated and footprint emission sensitivity plots (Figure 2 [*Fischer et al.*, 2006]).

[12] Because of the short sampling intervals (2 hours), each mist chamber sample was categorized by a single transport sector. The longer-duration aerosol samples were grouped by the predominant transport sector. If air was consistently transported from a single sector for greater than 75% of the sampling interval, then that sample was operationally categorized by that sector. This procedure represented a compromise between the limitation associated with the relatively long aerosol sampling intervals and the objective of interpreting transport regimes in terms of associated particulate NH_4^+ concentrations. This criterion allowed 44 of 60 aerosol samples to be classified into one of the six transport sectors. The longer-duration aerosol samples were associated with multiple paired mist chamber samples. To evaluate multiphase variability as a function of transport sector, the paired gas phase data were averaged over the period of each aerosol sampling interval; data for overlapping gas phase samples at the beginning and end of each aerosol sampling interval were weighted proportionately. Daily weather maps from the Department of Commerce (http://www.hpc.ncep.noaa.gov/dailywxmap/) were visually inspected to further interpret the role of air mass history and, specifically, the potential importance of scavenging and deposition via precipitation in fetch regions on the chemical characteristics of sampled air.

2.5. Calculations

[13] Dry-deposition fluxes of particulate NH_4^+ and the phase partitioning of NH_3 vary as functions of aerosol liquid water content (LWC) and pH [*Keene et al.*, 2004].

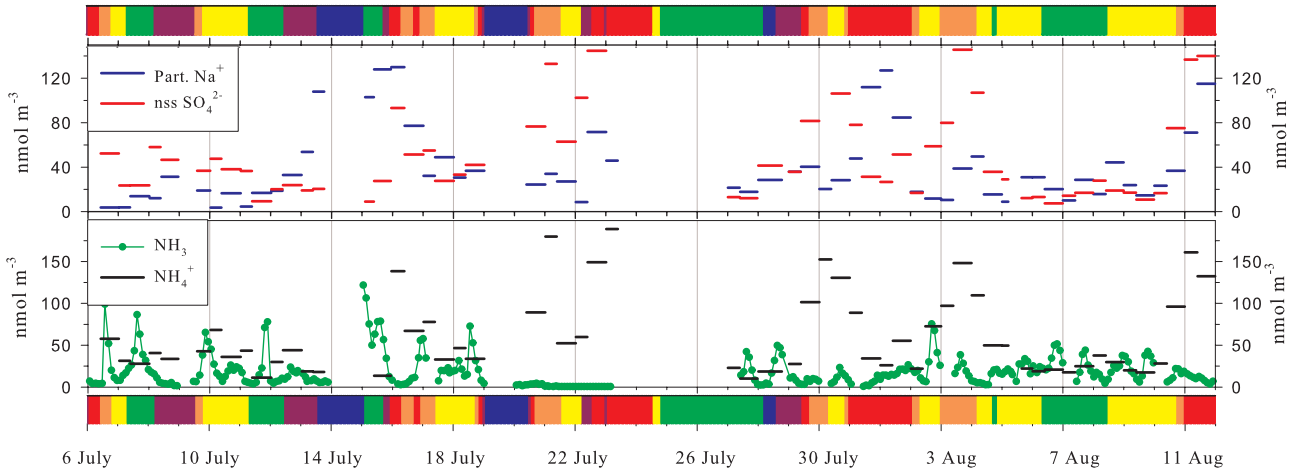

Figure 3. Time series of (top) Na^+ and nss SO_4^{2-} concentrations and (bottom) gaseous NH_3 and particulate NH_4^+ concentrations. Bars depict corresponding source regions based on the color scheme in Figure 2. Tick marks on the *x* axis are at 0000 UTC. ICARTT field operations were suspended between 23 July and 27 July.

LWCs were estimated on the basis of hygroscopicity models for NaCl [*Gerber*, 1985] and NH_4HSO_4 [*Tang and Munkelwitz*, 1994] following *Keene et al.* [2002a]. Aerosol pHs were inferred from the measured phase partitioning of HCl [*Keene et al.*, 2004].

[14] Dry-deposition fluxes of size-resolved particulate NH_4^+ to the surface ocean were modeled on the basis of the measured NH_4^+ concentration and corresponding GMD for each size fraction, wind velocity, air temperate, and RH following *Hummelshøj et al.* [1992]. The laminar sublayer was assumed to be at 98% RH [*Lewis and Schwartz*, 2004] and the corresponding GMD for a given size fraction in the sublayer was based on the measured ionic composition and the hygroscopicity models mentioned above.

[15] Dry-deposition fluxes of gaseous NH_3 to the surface ocean were modeled on the basis of the measured mixing ratios, wind speed, air temperature, and surface-seawater temperature following *Valigura* [1995]. This approach assumes no limit on gas solubility in the surface seawater. Although solubility limitations of this nature may be important for heavily polluted estuarine and nearshore coastal waters [e.g., *Larsen et al.*, 2001], available evidence suggests that such limitations are not significant in offshore coastal waters along the eastern seaboard during summer [e.g., *Russell et al.*, 2003]. Reported values of NH_4^+ concentrations for the surface of the Gulf of Maine during summer range from 0.01 μM to 0.07 μM [*Townsend*, 1998; *Runge and Jones*, 2003]. Assuming that these data are representative of surface waters surrounding Appledore, the corresponding calculated equilibrium gas phase concentrations based on an assumed pH of 8.0 [*Butler*, 1982] range from 9 to 63 pptv of NH_3. Only 2% to 7% of the ambient gas phase concentrations during the ICARTT campaign were less than or equal to these equilibrium gas phase concentrations. In addition, dry-deposition fluxes of NH_3 associated with the lowest 7% of ambient NH_3 concentrations accounted for less than 3% of the dry-gaseous flux. On the basis of the above, we infer that solubility limitations on the NH_3 dry-deposition fluxes were unimportant.

3. Results and Discussion

3.1. Summary of Measurements

[16] NH_3 and NH_4^+ concentrations during this study varied over large ranges (Figure 3 and Table 2). Median concentrations of NH_3 and NH_4^+ were similar to those measured at other locations in eastern New England but generally less than those at coastal locations in the mid-Atlantic region of the eastern U.S. (Table 3). These differences reflect the relatively closer proximity of the southern sites to intensive agricultural activities (commercial poultry and hog production, fertilizer applications, etc.) and associated NH_3 emissions in the mid-Atlantic region [*Russell et al.*, 2003].

Table 2. Summary Statistics for NH_3 and NH_4^+ Measured During This Campaign

Constituent	Maximum, nmol m^{-3}	Minimum, nmol m^{-3}	Average, nmol m^{-3}	Median, nmol m^{-3}	Number of Samples
NH_3	122	<0.4	19.6	14.3	310
NH_4^+[a]	189	10.2	60.8	42.9	60
Total NH_3[b]	181	29.3	73.2	52.3	44

[a] NH_4^+ corresponds to the sum over all impactor stages.
[b] Total NH_3 refers to the subset of paired particulate NH_4^+ and gaseous NH_3 data that were classified by source region (see section 2).

Table 3. Median Concentrations of Inorganic Atmospheric Nitrogen Species Measured in the Coastal and Near-Coastal Zone of the Northeastern and Mid-Atlantic United States

Location	Time Period	NH_3, nmol m^{-3}	NH_4^+, nmol m^{-3}	HNO_3, nmol m^{-3}	NO_3^-, nmol m^{-3}	Reference
Acadia National Park, Maine	summer 2004		43.1			CASTNET [*Environmental Protection Agency (EPA)*, 2006]
New Castle, New Hampshire	summer 1997		45.6	21.4	9.3	*Jordan et al.* [2000]
Woodstock, New Hampshire	summer 2004		38.3			CASTNET [*EPA*, 2006]
Appledore Island, Maine	6 Jul to 12 Aug 2004	14.3	42.9	23.0	11.3	this study/*Fischer et al.* [2006]
Harvard Forest, Massachusetts	1991–1995	10.0		16.8		*Lefer et al.* [1999]
Harvard Forest, Massachusetts	summers only 1991–1995		35.5		6.3	*Lefer and Talbot* [2001]
Dorchester, Maryland	summer 2004		133			CASTNET [*EPA*, 2006]
Lewes, Delaware	31 Jul to 13 Aug 2000	76.2	69.6	22.5	33.1	*Russell et al.* [2003]
Kinston, North Carolina	16 May to 31 Dec 2000	106	62.2	2.5	15.2	*Walker et al.* [2004][a]
Clinton, North Carolina	summers only 1998–1999	54.8	142			*Robarge et al.* [2002]
Clinton, North Carolina	1 Jan to 31 Dec 2000	260	93.6	8.9	22.5	*Walker et al.* [2004][a]
Morehead City, North Carolina	17 Jan to 19 Dec 2000	25.9	48.6	2.2	9.4	*Walker et al.* [2004][a]
Beaufort, North Carolina	summer 2004		61.4			CASTNET [*EPA*, 2006]

[a]Averages for median daytime and nighttime concentrations.

[17] When comparing data from different coastal or marine sites, it is important to recognize that a bulk sampling protocol such as that employed by the Clean Air Status and Trends Network (CASTNET) may not reliably quantify particulate phase concentrations for compounds with pH-dependent solubilities such as NH_3. The pH of the bulk mix of super-μm sea-salt and sub-μm sulfur aerosols is typically greater than that of the sub-μm aerosol size fractions with which most NH_4^+ is associated in the atmosphere [*Keene et al.*, 1990]. The higher pH results in supersaturation of bulk aerosol mixture relative to ambient NH_3 vapor, subsequent volatilization of NH_3, and associated negative artifacts in measured NH_4^+. Because of this effect, reported NH_4^+ concentrations that are based on analysis of aerosol sampled in bulk at coastal or open ocean locations should be considered lower limits.

[18] The time series data for NH_3 indicate a fairly consistent pattern of higher concentrations during the day (median for all values = 419 pptv) and lower at night (median for all values = 225 pptv). To characterize relative diel variability, NH_3 concentrations measured during each individual day (based on the midpoint of the sampling interval) were normalized to a common scale ranging from 0 to 1 by subtracting the minimum for the day and then dividing by the range for the day. The ranked values for every day were then binned into twelve 2-hour increments (e.g., 2300 to 0100; 0100 to 0300, etc.) and plotted (Figure 4). On the basis of median values, NH_3 peaked around local noon and decreased to minimum values near

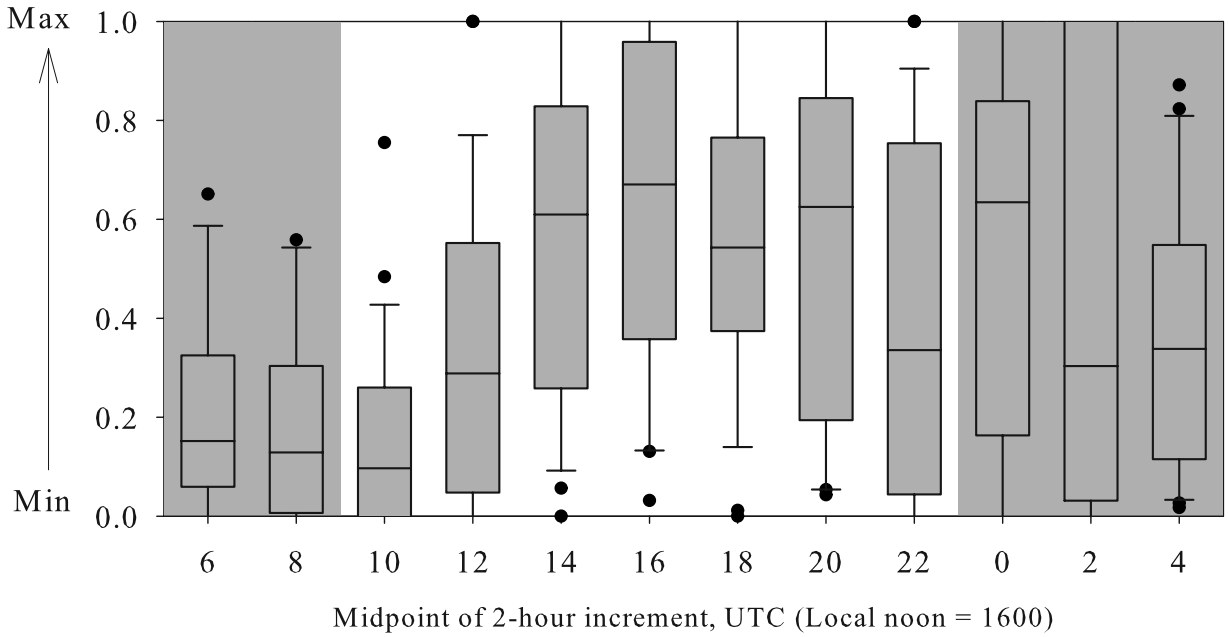

Figure 4. Normalized diel cycle of gaseous NH_3. The shaded area indicates night. Boxes depict 25th, 50th, and 75th percentiles; whiskers depict 10th and 90th percentiles. Extreme values are plotted individually.

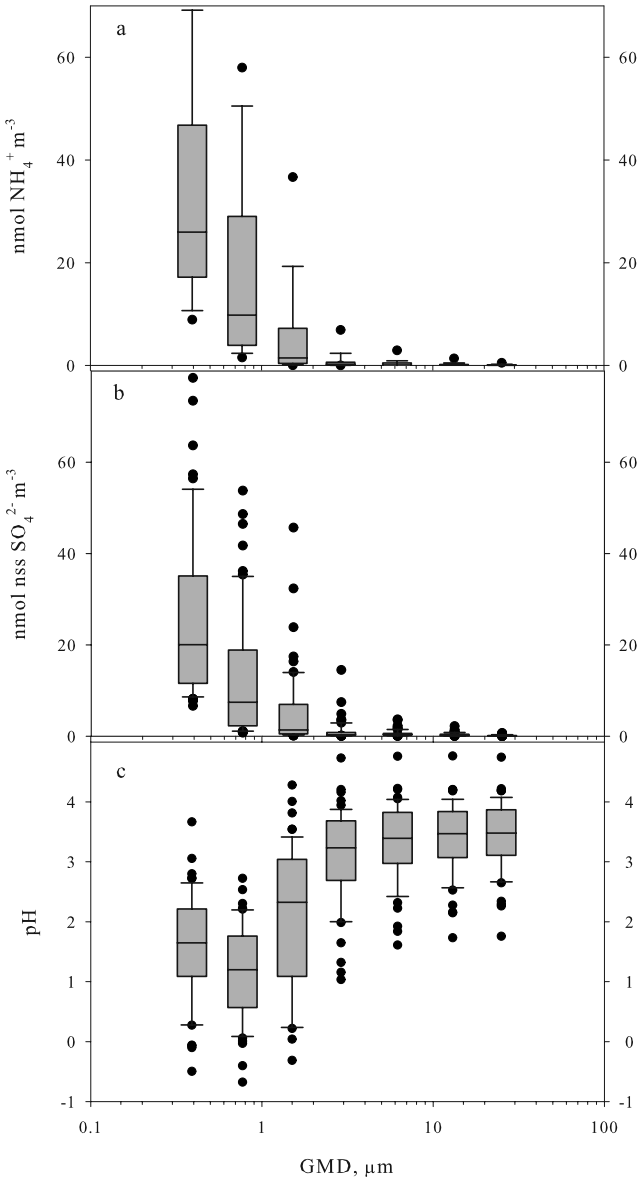

Figure 5. Size distributions of particulate (a) NH_4^+, (b) nss SO_4^{2-}, and (c) pH. The maximum concentration for NH_4^+ associated with the smallest size fraction (off scale) is 118 nmol m^{-3}.

dawn. Higher concentrations during the midday may be explained in part by the temperature dependence of NH_3 emissions sources [*Dentener and Crutzen*, 1994]. However, the depth of the mixed layer over the upwind continent also varies over diel cycles in response to surface heating [*Arya*, 2001] and thereby contributes to variability in the composition of near-surface air sampled at Appledore. At night, total NH_3 in the relatively shallow mixed layer is depleted via dry deposition to the surface. As the depth of the mixed layer increases in response to heating following sunrise, air from aloft that was not depleted by nocturnal deposition is entrained into the mixed layer, which contributes to rising concentrations in near-surface air during morning.

[19] Between 20 and 23 July, concentrations of NH_3 remained consistently near or below the detection limit; virtually all total NH_3 was in the form of NH_4^+ (Figure 3). These unusually low NH_3 concentrations were associated with a major pollution episode as indicated by some of the highest concentrations of nss SO_4^{2-} (Figure 3) and lowest aerosol pHs for the two smallest size fractions (GMD 0.77 μm fraction ranged from -0.68 to 0.72 and GMD 0.39 μm fraction ranged from -0.50 to 0.28) during the campaign. High aerosol acidity favors partitioning of NH_3 with the particulate phase [*Keene et al.*, 2004], which is consistent with these observations. In addition, the highest HNO_3 mixing ratio (7546 pptv) [*Fischer et al.*, 2006] and one of the highest HCl mixing ratios (3144 pptv) [*Keene et al.*, 2007] measured during the campaign also occurred during this period. The influence of acidic pollutant aerosol on NH_3 phase partitioned is addressed in more detail below.

[20] Figure 5a depicts the distribution of size-resolved NH_4^+ during this campaign. The highest concentrations of both NH_4^+ and nss SO_4^{2-} (Figure 5b) were associated with sub-μm size fractions. These size fractions also exhibited the highest aerosol acidities (Figure 5c). These relationships are consistent with those observed elsewhere (e.g., see citations in Table 3 and references therein) and reflect the pH dependence of NH_3 phase partitioning (discussed in more detail below).

3.2. Chemical Composition Versus Air Mass Source Region

[21] On the basis of median values, the concentrations of particulate NH_4^+, total NH_3, and nss SO_4^{2-} varied substantially among source regions with highest values associated with the more polluted midwest and southwest transport regimes (Figure 6). The nonparametric Median Test was employed to assess the null hypothesis that the independent distributions for the subsets of total NH_3 data corresponding to the six source regions are from populations with the same median. The null hypotheses for the midwest and the southwest urban sectors were rejected at 95% confidence. Two factors contribute to the differences in total NH_3 between transport regions. First, regional emissions inventories indicate greater anthropogenic sources for NH_3 (primarily agricultural activities including livestock farming and fertilizer application) in the midwest and southwest sectors relative to the other transport sectors [e.g., *Bouwman et al.*, 1997]. Second, as discussed in more detail below, the higher concentrations of acidic S aerosol associated with air transported from the more polluted midwestern and southwestern sectors leads to the partitioning of larger fractions of total NH_3 with sub-μm aerosols (Figure 7). Relative to gas phase NH_3, sub-μm size fractions have lower dry-deposition velocities (Figure 8) and, thus, longer atmospheric lifetimes against deposition.

[22] To evaluate the importance of transport from the more polluted midwest and southwest sectors (N = 14) relative to the cleaner sectors (N = 30) as a source for total NH_3 in coastal New England, the median values for the combined polluted (133 nmol m^{-3}) and the combined clean sectors (52 nmol m^{-3}) were weighed on the basis of the corresponding frequencies of transport from those sectors (0.32 and 0.68 respectively). These weighted contributions indicate that the relatively less frequent transport from the midwest and southwest sectors accounted for 55% of the

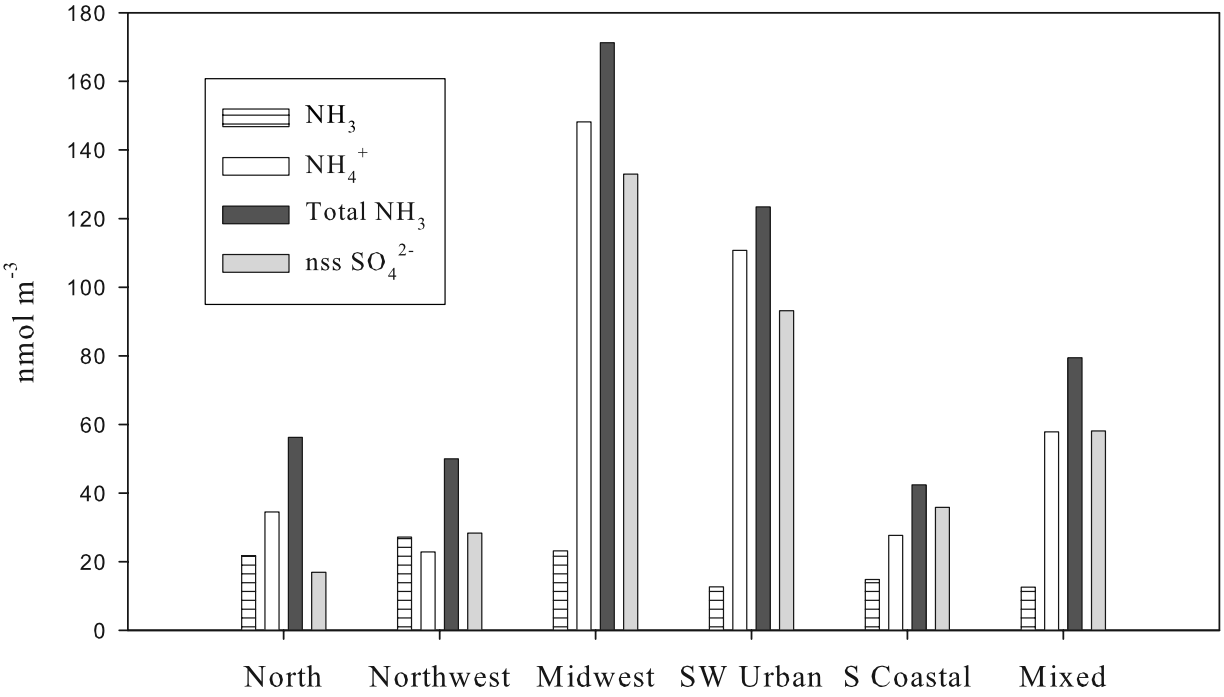

Figure 6. Median concentrations of NH_3, NH_4^+, total NH_3, and nss SO_4^{2-} as a function of source region. NH_3 concentrations were averaged over each aerosol sampling interval (see text); the numbers of paired aerosol and averaged NH_3 data for the north, northwest, midwest, southwest, south coastal, and mixed sectors were 10, 15, 5, 9, 5, and 16, respectively. Because aerosol sampling was suspended during the frequent periods of precipitation associated with easterly flow, no paired data are available for the marine sector.

median total NH_3 concentration in near surface air during the experiment.

[23] During two periods (17 July and 31 July), flow from the southwest was associated with relatively low concentrations of total NH_3 and nss SO_4^{2-} (<40 nmol m^{-3} each, Figure 7a). Each of these sampling periods was preceded by widespread precipitation over the southwest source region that persisted for several days (see http://www.hpc.ncep.noaa.gov/dailywxmap). This evidence suggests that precipitation scavenged these air parcels during transport thereby accounting for the relatively lower concentrations measured at Appledore.

3.3. Phase Partitioning

[24] The phase partitioning of NH_3 with deliquesced aerosol solutions is controlled primarily by the thermodynamic properties of the system expressed as follows:

$$NH_{3g} \overset{K_H}{\leftrightarrow} [NH_{3aq}] \overset{K_b}{\leftrightarrow} [NH_4^+] + K_w/[H^+] \quad (1)$$

where K_H and K_b are the temperature-dependent Henry's Law (62 M atm^{-1}) and dissociation constants (1.8×10^{-5} M), respectively, for NH_3 and K_w is the ion product of water (1.0×10^{-14} M) [*Chameides*, 1984]. It is evident that for a given amount of total NH_3 in the system, higher aqueous concentrations of particulate H^+ will shift the partitioning of NH_3 toward the condensed phase. Consequently, under the more polluted conditions characterized by higher concentrations of acidic S aerosol, the ratio of NH_3 to NH_4^+ decreased (Figures 6 and 7). It also follows that for a multiphase system such as this in which aerosol acidity varies as a function of particle size, NH_3 will partition preferentially with the more acidic sub-μm size fractions as is evident in our measurements (Figures 5 and 7). In addition, because virtually no NH_3 partitions with super-μm sea-salt size fractions under these conditions (Figure 5), the chemical processing of sea salt and NH_3 in polluted coastal air is largely decoupled. The large surface-to-volume ratios associated with the sub-μm aerosol size fractions facilitate rapid rates of equilibration (seconds to minutes) [*Meng and Seinfeld*, 1996] and, consequently, NH_3 phase partitioning is near thermodynamic equilibrium under most conditions.

[25] Although concentrations of total NH_3 were positively correlated with nss SO_4^{2-} (Figure 7a), ratios of NH_3 to NH_4^+ were negatively correlated (Figure 7c) because of the higher aerosol acidities (Figure 7b), greater aerosol volumes per unit volume of air (as indicated by nss SO_4^{2-}), and associated influences on NH_3 phase partition (relationship 1). Consequently, the concentrations of NH_3 vapor were not correlated with nss SO_4^{2-} (Figure 7d).

3.4. Dry Deposition

[26] The modeled dry-deposition velocities of gaseous NH_3 to the ocean surface were substantially greater than those for the sub-μm aerosol size factions (Figure 8) with which most NH_4^+ was associated (Figure 5). Because the presence of high concentrations of acidic S aerosols in air transported from midwest and southwest shifted NH_3 partitioning toward the longer-lived particulate phase (Figure 7), chemical interaction with acidic pollutant aerosols effectively

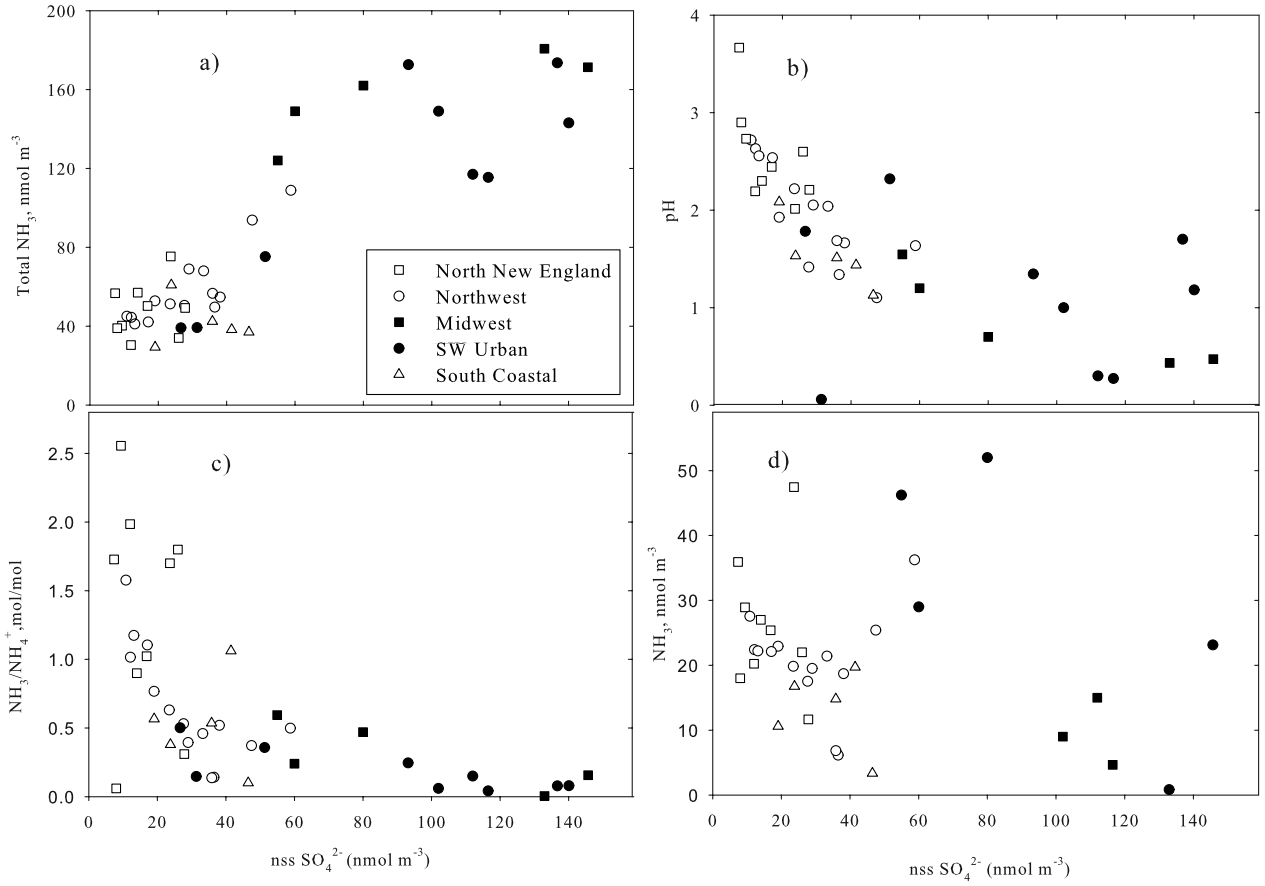

Figure 7. (a) Total NH_3, (b) pH of GMD 0.39 μm-size fraction, (c) molar ratio of gaseous NH_3 to particulate NH_4^+, and (d) gaseous NH_3 versus nss SO_4^{2-}.

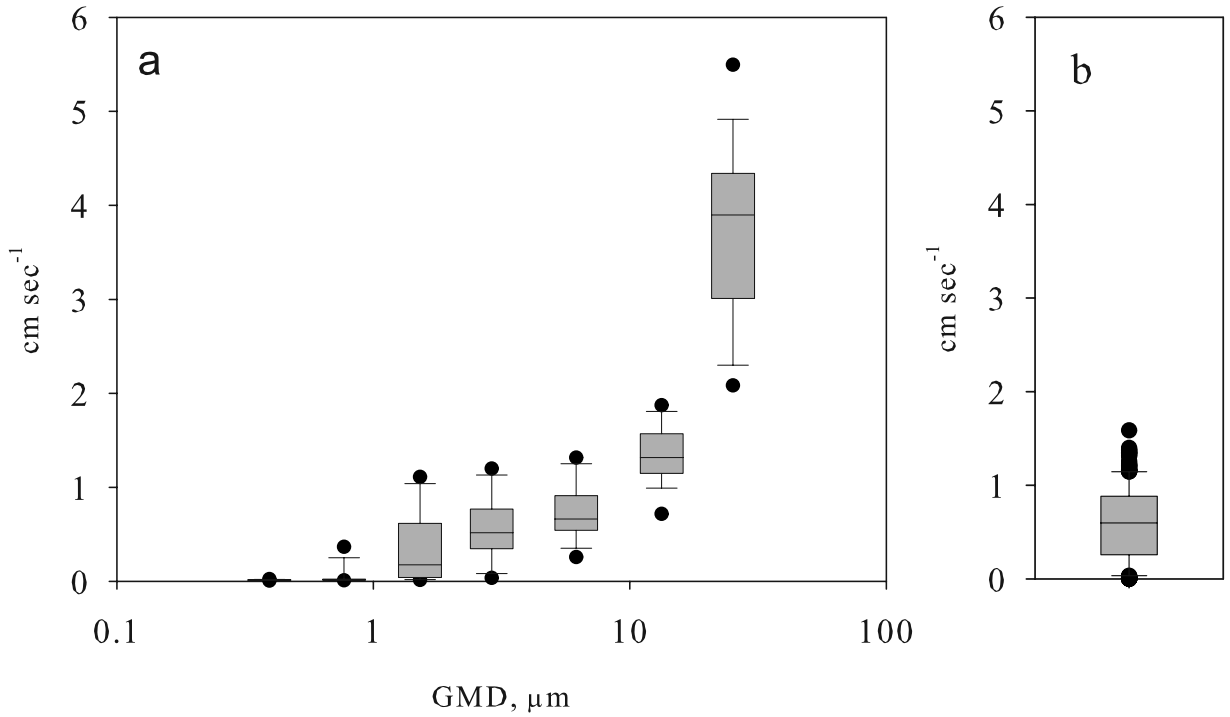

Figure 8. Deposition velocities for (a) size resolved particulate NH_4^+ and (b) gasesous NH_3.

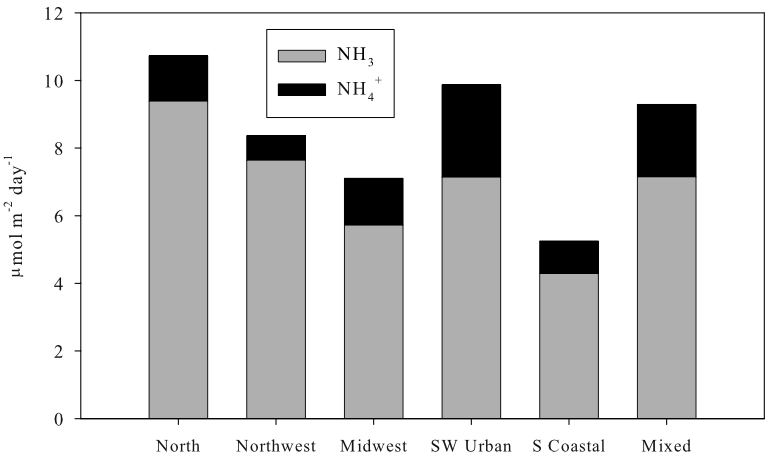

Figure 9. Median dry-deposition fluxes of NH_3 and NH_4^+ associated with transport from each source region.

increased the atmospheric lifetime of total NH_3 against dry deposition. This shift has important consequences for NH_3 cycling. Because gaseous NH_3 dominates the dry-deposition flux of total NH_3 (Figure 9), processes that influence NH_3 phase partition (primarily interaction with pollutant nss SO_4^{2-}) may be more important than the corresponding emission fluxes of NH_3 in controlling the dry deposition of total NH_3. For example, on the basis of median values for different transport sectors, relatively low concentrations of total NH_3 associated with the northerly transport sector (56.3 nmol m^{-3}, Figure 6) sustained the highest dry-deposition fluxes of total NH_3 (10.7 μmol m^{-2} day^{-1}, Figure 9). In contrast, the significantly higher (factor of 3) concentrations of total NH_3 associated with the more polluted midwest transport section (Figure 6) sustained lower (30%) dry-deposition fluxes of total NH_3 (Figure 9). The nonparametric Median Test was employed to assess the null hypothesis that the independent distributions for the subsets of total NH_3 dry-deposition fluxes corresponding to the six source regions are from populations with the same median. The null hypotheses were accepted for all subsets at 95% confidence.

[27] Assuming steady state, a well mixed boundary layer over the upwind continent of 1000 m depth, and no precipitation, the median concentrations and dry-deposition fluxes of total NH_3 discussed above correspond to atmospheric lifetimes against dry-deposition of ~24 and ~13 days, respectively, for air transported from the midwest and southwest sectors. The corresponding atmospheric lifetimes of total NH_3 in air transported from the north, northwest, and south coastal regions were ~5, ~6, and ~8 days, respectively. It is evident from the above that pollutant aerosol substantially increased the atmospheric lifetime of total NH_3 against dry deposition. However, the actual atmospheric lifetimes of total NH_3 may diverge substantially from those in the above example as a result of wet deposition, variability in the depth of the mixed layer, and transport of continental outflow above the marine boundary layer [e.g., *Neuman et al.*, 2006].

[28] The relatively longer atmospheric lifetime of total NH_3 against dry deposition under more polluted conditions implies that, on average, total NH_3 would accumulate to higher atmospheric concentrations under these conditions and also be subject to atmospheric transport over longer distances. Consequently, the importance of removal via wet relative to dry deposition would also increase. It follows that the sporadic nature of precipitation would contribute to greater heterogeneity in NH_3 deposition fields and potential ecological responses downwind of major S-emission regions.

3.5. Wet Versus Dry Deposition

[29] The relative average concentrations of individual inorganic N species and the corresponding dry-deposition fluxes are compared in Figures 10a and 10b. Each average flux corresponds to the integrated flux over all sampling intervals divided by the number of sampling days. Organic N was not quantified as part of this study, but available evidence suggests that it accounts for a relatively minor fraction of atmospheric nitrogen deposition in this region [*Keene et al.*, 2002b]. Although particulate NH_4^+ accounted for almost half of the N associated with these inorganic species in ambient air, it contributed only 11% of the corresponding average dry-deposition flux. Dry fluxes were dominated by HNO_3 (19.4 μmol m^{-2} day^{-1}) followed by NO_3^- (10.0 μmol m^{-2} day^{-1}), NH_3 (9.3 μmol m^{-2} day^{-1}), and particulate NH_4^+ (5.0 μmol m^{-2} day^{-1}). The integrated average fluxes (Figure 10b) suggest that NH_3 accounted for 66% of the dry-deposition flux of total NH_3. In contrast, the median fluxes (Figure 9) suggest somewhat greater relative contributions of NH_3 ranging from 72% to 91%. These differences reflect the relatively greater contributions from extreme values to the integrated dry flux of particulate NH_4^+ versus that of NH_3. Similar relationships are evident in relative differences between median and average concentrations of NH_4^+ versus NH_3 (Table 2). The average concentration for particulate NH_4^+ is 60% greater than its median concentration whereas the average concentration of NH_3 is only 19% greater than its median. The median values provide useful statistics for characterizing and comparing the central tendencies of the populations. In terms of total N loadings, however, integrated fluxes that reflect contributions from extreme values are more relevant statistics.

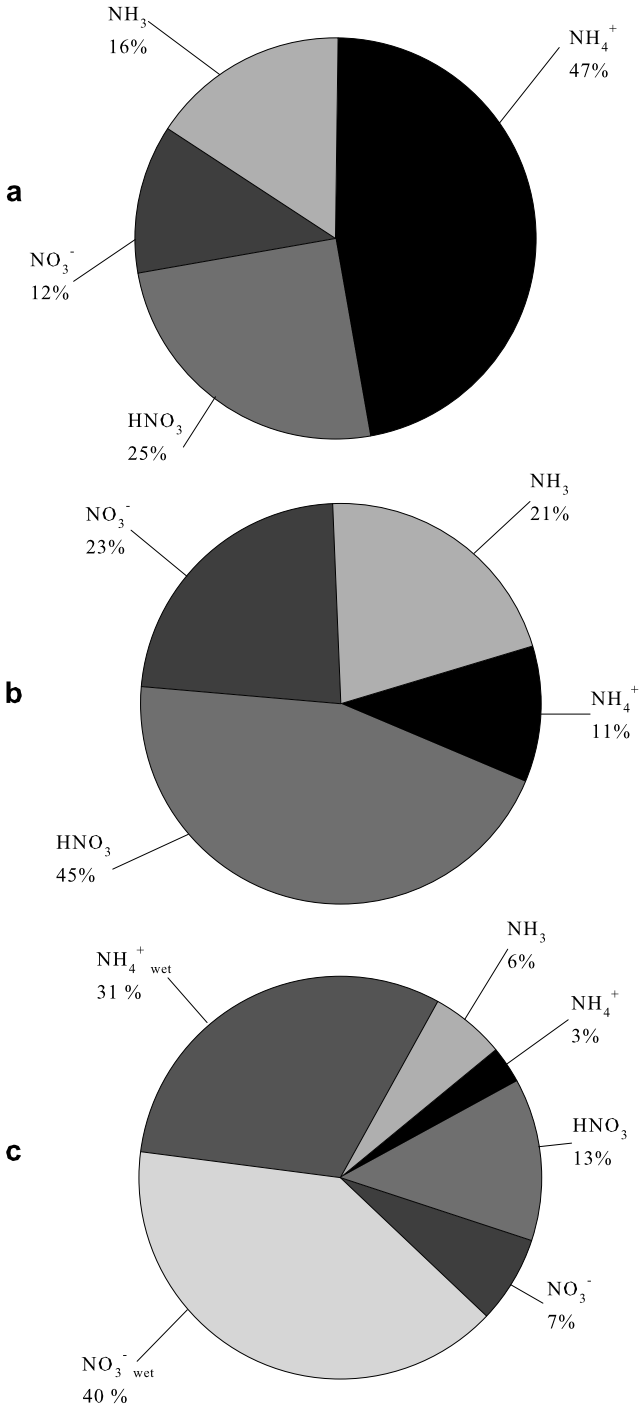

Figure 10. Relative contributions of NH_3, NH_4^+, HNO_3, and NO_3^- to (a) concentrations of major soluble inorganic N species in air, (b) corresponding dry-deposition fluxes, and (c) total (wet− + dry−) deposition fluxes. Dry-deposition rates correspond to averages for fluxes integrated over all gas and aerosol sampling periods.

[30] Wet-deposition fluxes of NH_4^+ and NO_3^- over the course of the experiment were quantified at Casco Bay, Maine (about 50 km N of the Appledore Island), by the National Atmospheric Deposition Program (http://nadp.sws.uiuc.edu/). Assuming that the averages for wet fluxes for NH_4^+ and NO_3^- at this site (31.5 and 55.7 μmol m^{-2} day^{-1}, respectively) are representative of those at Appledore, the combined dry-deposition fluxes of NH_3, HNO_3 and particulate NH_4^+ and NO_3^- contributed 29% of the total (wet plus dry) deposition flux of inorganic N during the campaign (Figure 10c). Accounting for the contributions from the dry deposition of NH_3 explains much of the difference between the greater percentage contribution of dry to total N deposition estimated during this investigation relative to that previously reported for the same region (10% to 20%) by *Jordan and Talbot* [2000].

[31] In contrast to the results of this study (Figure 10c), dry deposition contributes a substantially higher percentage (43%) of the total deposition flux of atmospheric N at Lewes, Delaware, during summer [*Russell et al.*, 2003]. The lower fraction of gaseous NH_3 relative to particulate NH_4^+ at Appledore compared to Lewes (Table 3) contributed to these differences. The higher concentrations of pollutant S aerosol over coastal New England during summer lead to the partitioning of most total NH_3 with the particulate phase, which increased its atmospheric lifetimes against dry deposition and thereby, increased the relative importance of removal via wet versus dry pathways.

4. Conclusions

[32] 1. Because of the pH-dependence of NH_3 phase partitioning, particulate NH_4^+ was associated almost exclusively with highly acidic sub-μm aerosol size fractions, which have long atmospheric lifetimes against deposition (many days) relative to NH_3 vapor (less than one day). Because virtually no NH_4^+ partitions with the relatively less acidic sea-salt size fractions, the cycling of sea salt and NH_3 in polluted coastal air are largely decoupled.

[33] 2. The dry-deposition flux of total NH_3 was dominated by gaseous NH_3.

[34] 3. Air transported from the cleaner northern and northwestern sectors typically contained relatively lower concentrations of total NH_3 and particulate nss SO_4^{2-} and H^+. Consequently, total NH_3 partitioned roughly equally between gaseous NH_3 and particulate NH_4^+ and, thus, deposited relatively rapidly to the surface.

[35] 4. Air transported from the southwest and midwest typically contained substantially higher concentrations of total NH_3 and particulate nss SO_4^{2-} and H^+. Consequently, total NH_3 partitioned primarily as particulate NH_4^+ and, thus, deposited relatively slowly to the surface.

[36] 5. The shift in phase partitioning from NH_3 to particulate NH_4^+ associated with the presence of pollutant S aerosol increased the atmospheric lifetime of total NH_3, which we infer led to higher atmospheric concentrations, transport over longer distances from sources, an increase in the relative importance of removal via wet versus dry deposition pathways, greater heterogeneity in N deposition fields, and greater potential ecological influences.

[37] 6. During this campaign, total NH_3 accounted for 32% of the dry-deposition flux of inorganic N to the coastal Gulf of Maine. The combined dry deposition of total NH_3 and wet deposition of NH_4^+ via precipitation contributed 40% of the corresponding total atmospheric N flux.

[38] **Acknowledgments.** We thank J. Moody and J. Galloway at the University of Virginia (UVA) and the anonymous reviewer for helpful

comments on the manuscript. The Shoals Marine Laboratory provided outstanding logistical support, R. Talbot and the AIRMAP Program at the University of New Hampshire (UNH) shared facilities and data, Plymouth State University archived HYSPLIT back trajectories for the program, and all participants contributed to an intellectually stimulating and thoroughly enjoyable field campaign. Principal financial support was provided by the National Science Foundation through awards to UVA (ATM 0401628) and UNH (ATM 0401622). Additional support was provided by NOAA through contracts NA03OAR4600122 and NA04OAR4600154 to UNH. This paper is contribution 133 to the Shoals Marine Laboratory.

References

Arya, S. P. (2001), *Introduction to Micrometeorology*, 2nd ed., Elsevier, New York.

Bouwman, A. F., D. S. Lee, W. A. H. Asman, F. J. Dentener, K. W. Van Der Hock, and J. G. J. Olivier (1997), A global high-resolution emission inventory for ammonia, *Global Biogeochem. Cycles*, *11*, 561–587.

Butler, J. N. (1982), *Carbon Dioxide Equilibria and Their Applications*, Addison-Wesley, Boston, Mass.

Castro, M. S., C. T. Driscoll, T. E. Jordan, W. G. Reay, W. R. Boynton, S. P. Seitzinger, R. V. Styles, and J. E. Cable (2001), Contribution of atmospheric deposition to the total nitrogen loads to thirty-four estuaries on the Atlantic and Gulf coasts of the Unites States, in *Nitrogen Loading in Coastal Water Bodies: An Atmospheric Perspective, Coastal Estuarine Stud.*, vol. 57, edited by R. A. Valigura et al., pp. 77–106, AGU, Washington D. C.

Chameides, W. L. (1984), The photochemistry of a remote marine stratiform cloud, *J. Geophys. Res.*, *89*, 4739–4755.

Dentener, F. J., and P. J. Crutzen (1994), A three-dimensional model of the global ammonia cycle, *J. Atmos. Chem.*, *19*, 331–369.

Draxler, R. R., and G. D. Rolph (2005), HYSPLIT (Hybrid Single-Particle Lagrangian Integrated Trajectory), NOAA Air Resour. Lab., Silver Spring, Md. (Available at http://www.arl.noaa.gov/ready/hysplit4.html)

Driscoll, C. T., et al. (2003), Nitrogen pollution in the northeastern United States: Sources, effects, and management options, *Bioscience*, *53*, 357–374.

Environmental Protection Agency (2006), Clean Air Status and Trends Network (CASTNET), Clean Air Markets, Washington, D. C. (Available at http://cfpub.epa.gov/gdm/index.cfm)

Fischer, E., A. A. P. Pzenny, W. Keene, J. Maben, A. Smith, A. Stohl, and R. Talbot (2006), Nitric acid phase partitioning and cycling in the New England coastal atmosphere, *J. Geophys. Res.*, *111*, D23S09, doi:10.1029/2006JD007328.

Galloway, J. N., G. E. Likens, and M. E. Hawley (1984), Acid precipitation: Natural versus anthropogenic components, *Science*, *226*, 829–831.

Galloway, J. N., et al. (2004), Nitrogen cycles: past, present, and future, *Biogeochemistry*, *70*, 153–226.

Gerber, H. E. (1985), Relative-humidity parameterization of the Navy aerosol model (NAM), *NRL Rep. 8956*, Natl. Res. Lab., Washington, D. C.

Hummelshøj, P., N. O. Jensen, and S. E. Larsen (1992), Particle dry deposition to a sea surface, in *Precipitation Scavenging and Atmosphere-Surface Exchange*, edited by S. E. Schwartz and W. G. N. Slinn, pp. 829–841, Taylor and Francis, Philadelphia, Pa.

Jordan, C. E., and R. W. Talbot (2000), Direct atmospheric deposition of water soluble nitrogen to the Gulf of Maine, *Global Biogeochem. Cycles*, *14*, 1315–1329.

Jordan, C. E., R. W. Talbot, and B. D. Keim (2000), Water-soluble nitrogen at the New Hampshire sea coast: HNO_3, aerosols, precipitation, and fog, *J. Geophys. Res.*, *105*, 26,403–26,431.

Keene, W. C., A. A. P. Pszenny, J. N. Galloway, and M. E. Hawley (1986), Sea-salt corrections and interpretation of constituent ratios in marine precipitation, *J. Geophys. Res.*, *91*, 6647–6658.

Keene, W. C., A. A. P. Pszenny, D. J. Jacob, R. A. Duce, J. N. Galloway, J. J. Schultz-Tokos, H. Sievering, and J. F. Boatman (1990), The geochemical cycling of reactive chlorine through the marine troposphere, *Global Biogeochem. Cycles*, *4*, 407–430.

Keene, W. C., J. R. Maben, A. A. P. Pszenny, and J. N. Galloway (1993), Measurement technique for inorganic chlorine gases in the marine boundary layer, *Environ. Sci. Technol.*, *27*, 866–874.

Keene, W. C., A. A. P. Pszenny, J. R. Maben, and R. Sander (2002a), Variation of marine aerosol acidity with particle size, *Geophys. Res. Lett.*, *29*(7), 1101, doi:10.1029/2001GL013881.

Keene, W. C., J. A. Montag, J. R. Maben, M. Southwell, J. Leonard, T. M. Church, J. L. Moody, and J. N. Galloway (2002b), Organic N in precipitation over eastern North America, *Atmos. Environ.*, *36*, 4529–4540.

Keene, W. C., A. A. P. Pszenny, J. R. Maben, E. Stevenson, and A. Wall (2004), Closure evaluation of size-resolved aerosol pH in the New England coastal atmosphere during summer, *J. Geophys. Res.*, *109*, D23307, doi:10.1029/2004JD004801.

Keene, W. C., J. Stutz, A. A. P. Pszenny, J. R. Maben, E. Fischer, A. M. Smith, R. von Glasow, S. Pechtl, B. C. Sive, and R. K. Varner (2007), Inorganic chlorine and bromine in coastal New England air during summer, *J. Geophys. Res.*, doi:10.1029/2006JD007689, in press.

Korhonen, P., M. Kulmala, A. Laaksonen, Y. Viisanen, R. McGraw, and J. H. Seinfeld (1999), Ternary nucleation of H_2SO_4, NH_3 and H_2O in the atmosphere, *J. Geophys. Res.*, *104*, 26,349–26,353.

Kulmala, M., L. Pirjola, and J. M. Mäkelä (2000), Stable sulphate clusters as a source of new atmospheric particles, *Nature*, *404*, 66–69.

Langford, A. O., F. C. Fehsenfeld, J. Zachariassen, and D. S. Schimel (1992), Gaseous ammonia fluxes and background concentrations in terrestrial ecosystems of the United States, *Global Biogeochem. Cycles*, *6*, 459–483.

Larsen, R. K., III, J. C. Steinbacher, and J. E. Baker (2001), Ammonia exchange between the atmosphere and the surface waters at two locations in the Chesapeake Bay, *Environ. Sci. Technol.*, *35*, 4731–4738.

Lefer, B. L., and R. W. Talbot (2001), Summertime measurements of aerosol nitrate and ammonium at a northeastern U. S. site, *J. Geophys. Res.*, *106*, 20,365–20,378.

Lefer, B. L., R. W. Talbot, and J. W. Munger (1999), Nitric acid and ammonia at a rural northeastern U. S. site, *J. Geophys. Res.*, *104*, 1645–1661.

Lewis, E. R., and S. E. Schwartz (2004), *Sea Salt Aerosol Production: Mechanisms, Methods, Measurements, and Models: A Critical Review*, *Geophys. Monogr. Series*, vol. 152, AGU, Washington, D. C.

Meng, Z., and J. H. Seinfeld (1996), Time scales to achieve atmospheric gas-aerosol equilibrium for volatile species, *Atmos. Environ.*, *30*, 2889–2900.

Meyers, T., J. Sickles, R. Dennis, K. Russell, J. Galloway, and T. Church (2001), Atmospheric nitrogen deposition to coastal estuaries and their watersheds, in *Nitrogen Loading in Coastal Water Bodies: An Atmospheric Perspective, Coastal Estuarine Stud.*, vol. 57, edited by R. A. Valigura et al., pp.53–76, AGU, Washington, D. C.

Neuman, J. A., et al. (2006), Reactive nitrogen transport and photochemistry in urban plumes over the North Atlantic Ocean, *J. Geophys. Res.*, *111*,D23S54, doi:10.1029/2005JD007010.

Nixon, S. W. (1995), Coastal marine eutrophication: A definition, social causes, and future concerns, *Ophelia*, *41*, 199–219.

Paerl, H. W. (1985), Coastal eutrophication in relation to atmospheric nitrogen deposition: Current perspectives, *Ophelia*, *41*, 237–259.

Paerl, H. W. (2002), Connecting atmospheric nitrogen deposition to coastal eutrophication, *Environ. Sci. Technol., Part A*, *36*, 323–326.

Paerl, H. W., L. R Dennis, and D. R. Whitall (2002), Atmospheric deposition of nitrogen: Implications for nutrient over-enrichment of coastal waters, *Estuaries*, *25*, 677–693.

Parrish, D. D., J. S. Holloway, M. Trainer, P. C. Murphy, G. L. Forbes, and F. C. Fehsenfeld (1993), Export of North American ozone pollution to the North Atlantic Ocean, *Science*, *259*, 1436–1439.

Pszenny, A. A. P., J. Moldanov, W. C. Keene, R. Sander, J. R. Maben, M. Martinez, P. J. Crutzen, D. Perner, and R. G. Prinn (2004), Halogen cycling and aerosol pH in the Hawaiian marine boundary layer, *Atmos. Chem. Phys.*, *4*, 147–168.

Robarge, W. P., J. T. Walker, R. B. McCulloh, and G. Murray (2002), Atmospheric concentrations of ammonia and ammonium at an agricultural site in the southeast United States, *Atmos. Environ.*, *36*, 1661–1674.

Runge, J. A., and R. J. Jones (2003), PULSE: A cooperative partnership for coastal ocean ecosystem monitoring in the Gulf of Maine, annual report, 20 pp., Cent. of Excellence for Coastal Ocean Obs. and Anal., Univ. of N. H., Durham.

Russell, K. M., W. C. Keene, J. R. Maben, J. N. Galloway, and J. L. Moody (2003), Phase partitioning and dry deposition of atmospheric nitrogen at the mid-Atlantic U. S. coast, *J. Geophys. Res.*, *108*(D21), 4656, doi:10.1029/2003JD003736.

Scudlark, J. R., and T. M. Church (1999), A comprehensive reexamination of the input of atmospheric nitrogen to the Rehoboth and Indian River estuaries, report, Cent. for Inland Bays and Del. Dep. of Nat. Resour. and Environ. Control, Dover, Del.

Seibert, P., and A. Frank (2004), Source-receptor matrix calculation with a Lagrangian particle dispersion model in backward mode, *Atmos. Chem. Phys.*, *4*, 51–63.

Stohl, A., C. Forster, S. Eckhardt, N. Spichtinger, H. Huntrieser, J. Heland, H. Schlager, S. Wilhelm, F. Arnold, and O. Cooper (2003), A backward modeling study of intercontinental pollution transport using aircraft measurements, *J. Geophys. Res.*, *108*(D12), 4370, doi:10.1029/2002JD002862.

Stohl, A., C. Forster, A. Frank, P. Seibert, and G. Wotawa (2005), Technical note: The Lagrangian particle dispersion model FLEXPART version 6.2, *Atmos. Chem. Phys.*, *5*, 2461–2474.

Strader, R., N. Anderson, C. Davidson (2004), CMU ammonia model, version 3.6, Carnegie Mellon Univ., Pittsburgh, Pa. (Available at http://www.cmu.edu/ammonia)

Tang, I. N., and H. R. Munkelwitz (1994), Water activities, densities, and refractive indices of aqueous sulfates and sodium nitrate droplets of atmospheric importance, *J. Geophys. Res.*, *99*, 18,801–18,808.

Townsend, D. W. (1998), Sources and cycling of nitrogen in the Gulf of Maine, *J. Mar. Syst.*, *16*, 283–295.

Valigura, R. A. (1995), Iterative bulk exchange model for estimating air-water transfer of HNO_3, *J. Geophys. Res.*, *100*(D12), 26,045–26,050.

Walker, J. T., D. R. Whiteall, R. Robarge, and H. W. Paerl (2004), Ambient ammonia and ammonium aerosol across a region of variable ammonia emission density, *Atmos. Environ.*, *38*, 1235–1246.

E. Fischer, Department of Atmospheric Sciences, University of Washington, Seattle, WA 98195, USA.

W. C. Keene and J. R. Maben, Department of Environmental Sciences, University of Virginia, Clark Hall, P.O. Box 400123, Charlottesville, VA 22904, USA. (wck@virginia.edu)

A. A. P. Pszenny, Institute for the Study of Earth, Oceans and Space, University of New Hampshire, Durham, NH 03824, USA.

A. M. Smith, Pollard Environmental, LLC, Richmond, VA 23233, USA.

A. Stohl, Norwegian Institute for Air Research, N-2027 Kjeller, Norway.